OPTOELECTRONICS AND ADVANCED MATERIALS – RAPID COMMUNICATIONS Vol. 3, No. 7, July 2009, p. 676 - 679

p-type ZnO nano-thin films prepared by oxidation of Zn_3N_2 deposited by rf magnetron sputtering

ZHANG JUN[a,b], SHAO LE-XI[a*]
[a]*School of Physics Science and Technology, Zhanjiang Normal university, Zhanjiang 524048, China*
[b]*School of Physical Science and Technology, Lanzhou University, Lanzhou 730000, China*

p-type ZnO:N thin films were prepared by thermal oxidation of RF magnetron sputtered Zn_3N_2 films on glass substrates. The effects of oxidation temperature on the structural, optical and electrical properties of the samples were investigated by X-ray diffraction (XRD), scanning electron microscopy (SEM), optical transmittance, photoluminescence (PL) and Hall effect measurements. XRD analyses revealed that Zn_3N_2 films entirely transformed into ZnO:N films after annealing Zn_3N_2 films in oxygen at 500 ^{o}C for 2 hours. Hall effect measurements confirmed p-type conduction in ZnO:N films with a low resistivity of 4.8 Ω·cm, a high hole concentration of 9.6×10^{18} cm^{-3} and a Hall mobility of 2.1 cm^2/Vs. the films are highly transparent in the visible region and the absorption edge blue shifts with increasing oxidation temperature from 450 – 550 ^{o}C. The films exhibited strong excitonic UV emission and weak deep-level emission. Our results demonstrate a promising approach to fabricate low resistivity p-type ZnO with high hole concentration.

(Received May 22, 2008; accepted July 20, 2009)

Keywords: **p**-type ZnO films, RF magnetron sputtering, XRD, Photoluminescence

1. Introduction

ZnO is an II-VI semiconductor with various interesting electrical, optical, acoustic and chemical properties due to its wide bandgap of 3.4 eV and a large exciton binding energy of 60 meV at room temperature [1-3]. ZnO, like GaN, will be important for blue and ultra-violet devices. ZnO has several advantages over GaN in this application range in its larger exciton binding energy and the ability to grow single crystal substrates. Other favorable aspects of ZnO include its broad chemistry leading to many opportunities for wet chemical etching, low power threshold for optical pumping, radiation hardness and biocompatibility. These properties of ZnO make it an ideal candidate for a variety of devices ranging from sensors through to ultra-violet laser diodes and nanotechnology-based devices such as displays [4-5].

Though ZnO already has many industrial applications owing to its piezoelectric properties and band gap in the near ultraviolet, the main obstacle to the development of ZnO has been the lack of reproducible and low-resistivity p-type ZnO. In recent years, many techniques have been widely employed to synthesize p-type ZnO films, such as molecular-beam epitaxy, chemical-vapor deposition, sputtering, spray deposition, diffusion, oxidation of Zn_3N_2 [5-8]. Recent theoretical and experimental studies show that nitrogen is a very promising p-type dopant, but its solubility in ZnO is low. Co-doping method and ion implantation have been used to improve nitrogen content in ZnO . Thermal oxidization of Zn_3N_2 also seems to be an effective approach to obtain p-type ZnO with high hole concentration. Recently, Li et al. prepared p-type ZnO:N by thermal oxidization of PECVD-deposited Zn_3N_2. However, low-resistivity p-type ZnO has not yet been obtained using this method [9-10].

In this paper, we report the preparation of low-resistivity p-type ZnO:N thin films by oxidization of RF magnetron sputtered Zn_3N_2 films on glass substrates. By controlling the oxidation temperature, p-type ZnO:N films with high hole concentrations and low resistivity were obtained.

2. Experimental procedure

Zn_3N_2 thin films were prepared on glass slice by reactive RF magnetron sputtering using pure zinc disk as target and Ar–N_2 as working gas. The substrates are ultrasonically cleaned in acetone and alcohol for 15min, respectively. Then, they are rinsed in distilled water and dried in flowing hot air. The metallic zinc with 99.999% purity was used as target with a diameter of 60 mm and a thickness of 4 mm. The sputtering chamber was evacuated below 2.5×10^{-4} Pa with a combination of turbo molecular pump and rotary pump. Ar and N_2 used as sputtering gas was introduced into the sputtering chamber through mass flow controllers. The flow rates of Ar and N_2 were regulated to 15 sccms. The working pressure was kept at 1.5 Pa. The target-substrate distance was maintained at 60 mm. A RF power supply of 200 W was used as a power source. Before deposition, the zinc target was pre-sputtered in argon atmosphere for about 15 min in order to remove the surface oxide layer of the target. During sputtering, N_2 was decomposed into nitrogen atoms and/or nitrogen ions. Either nitrogen atoms or nitrogen ions are very active, so Zn_3N_2 films could be deposited easily at substrate temperature over 100 ^{o}C. In this work, the substrate temperature was precisely controlled from 100 to 300 ^{o}C. The sputtering time was 30 min.

After deposition, the as-deposited films were transferred into a tube furnace filled with high purity O_2 for oxidation. The oxidization temperature was quickly elevated to 400 °C, 500 °C and 550 °C and kept at these temperatures for 2 hours, respectively. After oxidation, all the samples were cooled down to the ambient temperature in the furnace.

The as-deposited Zn_3N_2 films showed dark-gray color, and became transparent after annealing in oxygen. The thicknesses of the films were about 500nm evaluated by cross section SEM micrograph. To characterize the structural, optical and electrical properties of the samples, the crystal orientation was investigated using X-ray diffractometer (XRD). The surface morphology of the films was observed through a scanning electron microscope (SEM). Room temperature (RT) photoluminescence spectra (PL) were recorded by a spectrophotometer with excitation wavelength of 325 nm.

3. Results and discussion

Figs. 1 and 2 show the typical SEM images of as-deposited Zn_3N_2 films and the films oxidized at 500 °C. It can be seen that the as-deposited film is composed of uniform particles with micron size. After oxidation, the surface morphology of the films changes significantly and many nano-grains form on the surface of the films. The average diameter of nano-grains is estimated to be about 120 nm.

Fig. 3 shows the XRD patterns of the as-deposited films and the films oxidized at different temperatures. The as-deposited Zn_3N_2 sample has a cubic structure with (321) and (440) planes. After the oxidative annealing at 400 °C, all the diffraction peaks observed in Fig.2 can be ascribed to hexagonal polycrystalline ZnO phase and cubic Zn_3N_2. The samples exhibit a mixed structure. After the oxidative annealing at 500 °C for 2 h, no XRD peaks assignable to Zn_3N_2 phases are found in all the ZnO:N samples. These results indicate that the as-deposited Zn_3N_2 films are entirely transformed into the ZnO:N films by the oxidative annealing.

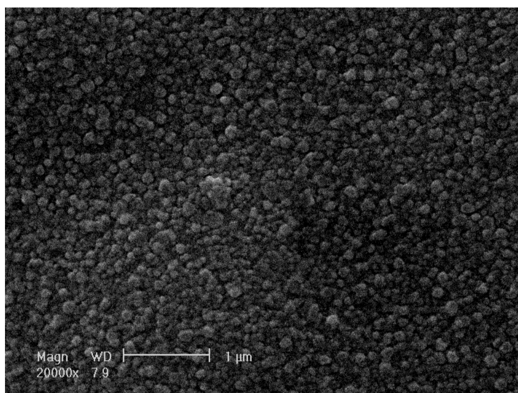

Fig. 1. SEM image of as-deposited film.

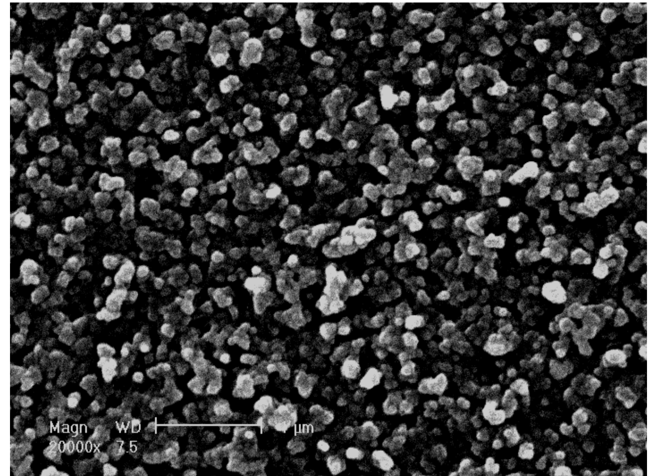

Fig. 2. SEM image of films oxidized at 500 ℃.

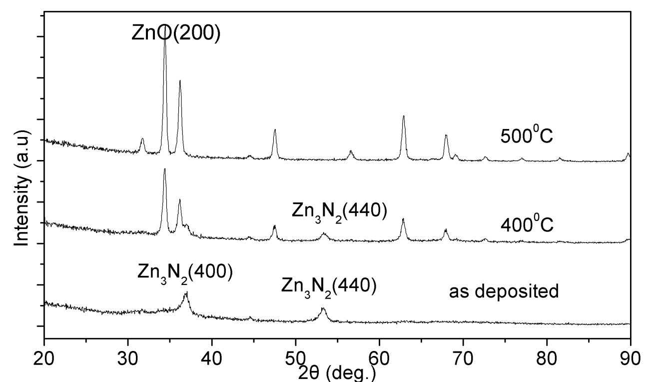

Fig. 3. XRD spectra of samples annealed at different temperatures and as-grown film.

The measurement of electrical properties including resistivity, carrier concentration, and Hall mobility was performed on the Hall effect measurement system (HEM2000) with a magnetic field strength of 0.5 T using the van der Pauw method at room temperature (RT). Before electrical measurements, silver spot electrodes were deposited on ZnO:N films and the ohmic contact between electrodes and films was confirmed. The measurement results were listed in Table 1. It can be seen that the samples oxidized at 400°C for 2 h still exhibited n-type conduction with a carrier concentration as high as $6.5\times10^{19}cm^{-3}$. This is due to the unfully oxidization of the as-deposited Zn_3N_2 films as revealed in XRD patterns. Further oxidative annealing at 500 °C for 2 h saw the p-type conversion in the samples. XRD analysis revealed that the as-deposited Zn_3N_2 films entirely transformed into ZnO:N films at this stage. Hall effect measurement results showed that the ZnO:N films had a low resistivity of 4.8 Ω·cm, a hole carrier concentration of $9.6\times10^{18}cm^{-3}$ and a Hall mobility of $2.1cm^2/Vs$. However, when the oxidation temperature exceeded 500°C, the carrier concentration and mobility of ZnO:N films decreased while the resistivity increased. This may be due to the out-diffusion of N acceptors at high annealing temperatures.

Table. 1. Electrical properties of ZnO:N films oxidized at different temperatures.

Oxidization temperature T(□)	Resistivity (Ω·cm)	Mobility (cm^2/ V·s)	Carrier concentration (cm^{-3})	Conductivity type
400	0. 56	0.83	-6.4947E+19	n
500	4.2	2.15	+9.6537E+18	p
550	103.6	1.32	+1.2012E+17	p

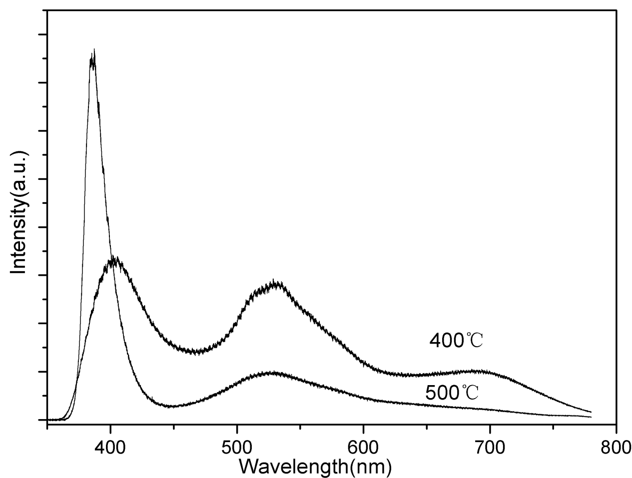

Fig. 4. RT PL spectra of ZnO:N films after oxidization at different temperatures.

Fig. 4 shows RT PL spectra of ZnO:N films after oxidization at different temperatures. The shape of all the spectra, similar to those reported by others, is featured by a near band edge (NBE) excitonic UV emission and a defect related deep level emission (DLE) in the visible region. It can be seen that NBE is dramatically enhanced after oxidative annealing at 500 ^{o}C while DLE is evidently decreased. This suggests an improvement of the ZnO:N crystallinity. In addition, a evident blueshift of NBE occurs after oxidative annealing at 500 ^{o}C, which may be attributed to the improvement of ZnO:N crystallinity.

Fig. 5 shows the absorption spectra of the films oxidized at different temperatures. It can be seen that the fundamental absorption edge locates at around 380 nm. The films are highly transparent in the visible region and the average transmittance is over 85%. The optical bandgaps can be determined from a conventional method. It is found that oxidation temperature has evident influences on the optical bandgaps of the films. The optical bandgap blueshifts with increasing the oxidation temperatures from 450 – 550 ^{o}C as shown in the inset of Fig. 5. For the films oxidized at 550 ^{o}C, the optical bandgap reaches 3.27eV. The blueshift of the optical bandgap can be attributed to the continuous decrease of Zn_3N_2 in the films as confirmed by XRD, which makes the films be more stoichiometric.

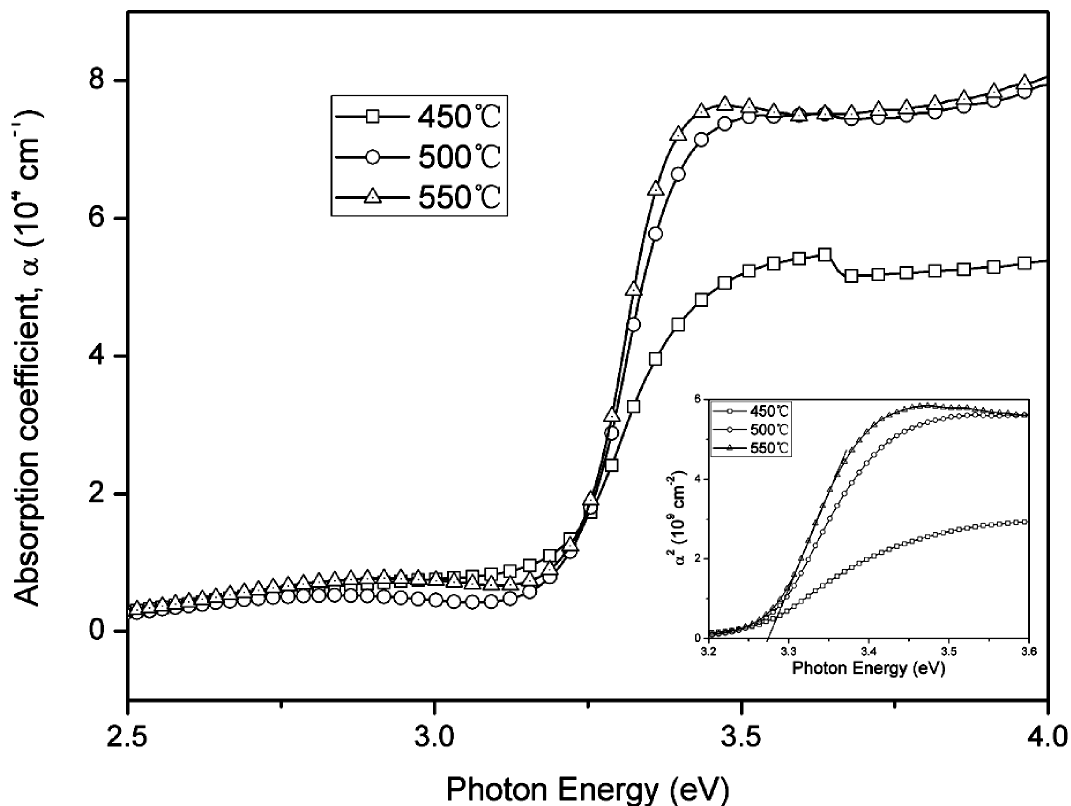

Fig. 5. Absorption spectra of the films oxidized at different temperatures.

4. Conclusions

It has been found that the sample oxidized at 400 °C for 2 h exhibits mixed structure with coexistence of cubic Zn_3N_2 and hexagonal ZnO. After oxidative annealing at 500 for 2 h the as-deposited Zn_3N_2 films entirely transform into ZnO:N films with excellent p-type electrical properties. The ZnO:N films possess a resistivity of 4.8 Ω·cm, a hole concentration of 9.6×10^{18} cm^{-3} and a Hall mobility of 2.1 cm^2/Vs. In addition, The ZnO:N films exhibit strong NBE and week DLE. This suggests that thermal oxidization of Zn_3N_2 is an very effective method to fabricate low-resistivity p-type ZnO with high hole concentration.

Acknowledgments

The authors would like to thank the National Natural Science Foundation of china under contract No. 10574106 and the Science & Technology Foundation of Zhanjiang Normal university for the financial supports.

References

[1] E. Przedzieck, E. Kamiska, I. Pasternak, A. Piotrowska, J. Kossut, Physical Review B **76**, 193303 (2007).
[2] M. Futsuhara, K. Yoshioka, O. Takai, Thin Solid Films **322**, 274 (1998).
[3] J. M. Bian, X. M. Li, C. Y. Zhang, W. D. Yu, X. D. Gao, Appl. Phys. Lett. **85**, 4070 (2004).
[4] Z. Ji, C. Yang, K. Liu, Z. Ye, J.Crystal Growth **253**, 239 (2003).
[5] Z.-Z. Ye, J.-G. Lu, H.-H. Chen, Y.-Z. Zhang, J. of Crystal Growth **253**, 258 (2003).
[6] D. C. Look, D. C. Reynolds, C. W. Litton, L. L. Jones, D. B. Eason, G. Cantwell, Appl. Phys. Lett. **81**, 1830 (2002).
[7] E. Kaminska, A. Piotrowska, J. Kossut, A. Barcz, R. Butkute, Solid State Communications **135**, 11 (2005).
[8] X.-L. Guo, H. Tabata, T. Kawai, J. Crystal Growth **223**, 135 (2001).
[9] V. Kambilafka, P. Voulgaropoulou, S. Dounis, E. Iliopoulos, M. Androulidaki, Thin Solid Films **515**, 8573 (2007).
[10] C. Wang, Z. Ji, K. Liu, Y. Xiang, Z. Ye, J. Cryst. Growth **259**, 279 (2003).

*Corresponding author: shaolxmail@163.com